A Patient-Specific Measurement Technique to Model Shoulder Joint Kinematics

C. Charbonnier[a,*], S. Chagué[a], F.C. Kolo[b], J.C.K. Chow[c], A. Lädermann[d,e]

[a] *Artanim Foundation, Medical Research Department, Geneva, Switzerland*
[b] *Rive Droite Radiology Center, Geneva, Switzerland*
[c] *Department of Geomatics Engineering, University of Calgary, Calgary, Canada*
[d] *Division of Orthopaedics and Trauma Surgery, La Tour Hospital, Geneva, Switzerland*
[e] *Faculty of Medicine, University of Geneva, Geneva, Switzerland*

* Corresponding author:
Address:
C. Charbonnier
Medical Research Department
Artanim Foundation
41b, route des Jeunes
1227 Carouge - Switzerland
Tel.: +41 (0)22 596 45 40
Fax: +41 (0)22 320 07 76
Email: caecilia.charbonnier@artanim.ch

Abstract

Background: Measuring dynamic in vivo shoulder kinematics is crucial to better understanding numerous pathologies. Motion capture systems using skin-mounted markers offer good solutions for non-invasive assessment of shoulder kinematics during dynamic movement. However, none of the current motion capture techniques have been used to study translation values at the joint, which is crucial to assess shoulder instability. The aim of the present study was to develop a dedicated patient-specific measurement technique based on motion capture and magnetic resonance imaging (MRI) to determine shoulder kinematics accurately.

Hypothesis: Estimation of both rotations and translations at the shoulder joint using motion capture is feasible thanks to a patient-specific kinematic chain of the shoulder complex reconstructed from MRI data.

Materials and Methods: We implemented a patient-specific kinematic chain model of the shoulder complex with loose constraints on joint translation. To assess the effectiveness of the technique, six subjects underwent data acquisition simultaneously with fluoroscopy and motion capture during flexion and empty-can abduction. The reference 3D shoulder kinematics was reconstructed from fluoroscopy and compared to that obtained from the new technique using skin markers.

Results: Root mean square errors (RMSE) for shoulder orientation were within 4° (mean range: 2.0° to 3.4°) for each anatomical axis and each motion. For glenohumeral translations, maximum RMSE for flexion was 3.7 mm and 3.5 mm for empty-can abduction (mean range: 1.9 to 3.3 mm). Although the translation errors were significant, the computed patterns of humeral translation showed good agreement with published data.

Discussion: To our knowledge, this study is the first attempt to calculate both rotations and translations at the shoulder joint based on skin-mounted markers. Results were encouraging and can serve as reference for future developments. The proposed technique could provide valuable kinematic data for the study of shoulder pathologies.

Level of evidence: Basic Science Study

Keywords: Shoulder kinematics, Glenohumeral translation, Global optimization, Motion capture, Fluoroscopy

1. Introduction

Measuring dynamic in-vivo shoulder kinematics is crucial to better understanding numerous pathologies and sport injuries, but remains a challenging problem due to the complicated anatomy and large range of motion. Unfortunately, the motion of the shoulder joints cannot be explored with standard Magnetic Resonance Imaging (MRI) or Computed Tomography (CT) because these are limited to static measurement and might therefore miss some specificities of dynamic motion. Fluoroscopy-based measurement provides sufficient accuracy for dynamic shoulder analysis [1], but uses ionizing radiation. Motion capture systems using skin-mounted markers are good solutions to determine shoulder kinematics non-invasively during dynamic movement [2, 3]. However, these systems are subject to soft tissue artifacts (STA) due to muscle contractions and skin sliding, causing the markers to move with respect to the underlying bone. In the upper extremity, the scapula is particularly affected. To solve this issue, several techniques were proposed such as the scapula locator device [4], the acromion marker cluster [5, 6] or the use of a large number of markers to track skin deformation and infer scapular motion [7].

Nevertheless, none of the current motion capture techniques have been used to study translation values at the shoulder joint. This information is crucial to assessing shoulder instability and to understanding many motion-related disorders (e.g., shoulder impingement). One reason for this lack is that studies using the current techniques concentrated either on analysis of a single shoulder bone (scapula) or on humeral motion relative to the thorax rather than to its proximal bone. Yet, it is important to consider the contribution of each bone in assessing shoulder kinematics, taking account of the whole kinematic chain of the shoulder complex from thorax to humerus via the clavicle and scapula, as this could help reduce overall STA error [8, 9]. Another important aspect is the ability to combine the anatomical and kinematic data of the patient: if the patient's anatomy (3D models) can be integrated into the kinematic model, the true bone axes and rotation center of the patient's actual shoulder can be used. Furthermore, this data enables direct assessment of the patient's anatomy in motion.

Our hypothesis was that both rotations and translations at the shoulder joint could be assessed on motion capture thanks to MRI reconstruction of the patient-specific kinematic chain of the shoulder complex. The purpose of this study was thus: (1) to develop a dedicated patient-specific measurement technique to determine shoulder kinematics accurately; (2) to assess the effectiveness of the technique by comparing the resulting 3D kinematics with that obtained by simultaneous X-ray fluoroscopy during functional activity.

2. Materials and Methods

2.1. Subjects

Six adult healthy males with no pathologic shoulder instability or limitation of range of motion were recruited (age = 39.6 ± 7.0 years, height = 181.1 ± 5.9 cm, weight = 81.6 ± 4.4 kg) for the study. Exclusion criteria were history of shoulder injury or shoulder surgery, and contraindications for MRI. The dominant arm (right arm, except for one subject) was used throughout testing. Ethical approval was gained from the local Institutional Review Board, and all participants gave their written informed consent.

2.2. MRI bone models

All subjects underwent MR shoulder arthrography to assess all images prospectively for rotator cuff and labral lesions (results not reported in this article). MRI was performed with a 1.5 T HDxT system (General Electric Healthcare, Milwaukee, WI, USA). A shoulder-dedicated surface coil was used. Three 3D MRI volumes were acquired: a cosmic 3D fast gradient echo sequence with fat saturation (section thickness 1.8 mm; no gaps; TR/TE ms 6.1/3.0; flip angle 45°) capturing from the acromion to approximately the mid-part of the scapula, a cosmic 3D fast gradient echo sequence (section thickness 4 mm; no gaps; TR/TE ms 5.7/2.8) capturing from the acromion to approximately the mid-shaft of the humerus, and a lava 3D fast gradient echo sequence (section thickness 5.2 mm; no gaps; TR/TE ms 3.7/1.7) capturing from the acromion to the elbow.

The MRI volumes were registered and manually segmented by a musculoskeletal radiologist (FCK) using ITK-SNAP software [10]. Based on the segmented contours, 3D models of the shoulder bones (humerus, scapula, clavicle and sternum) were reconstructed for each volunteer. Local coordinate systems (Fig. 1) were then established based on the definitions suggested by the International Society of Biomechanics [11] to represent the thorax, clavicle, scapula and humerus segments, using anatomical landmarks identified on the reconstructed bone models and MR images. The glenohumeral joint center was calculated using a sphere fitting method [12].

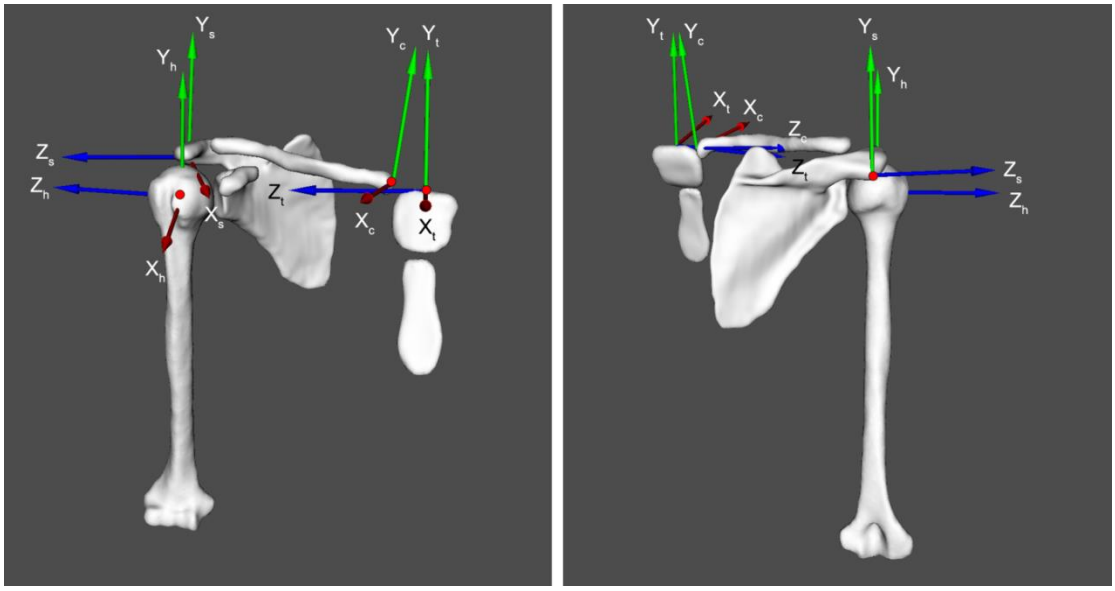

Figure 1: Bone coordinate systems for the thorax ($X_t\,Y_t\,Z_t$), clavicle ($X_c\,Y_c\,Z_c$), scapula ($X_s\,Y_s\,Z_s$) and humerus ($X_h\,Y_h\,Z_h$).

2.3. Data collection

Participants were equipped with spherical retroreflective markers (Fig. 2) placed directly on the skin. Four markers (Ø14 mm) were attached to the thorax (sternal notch, xyphoid process, C7 and T8 vertebra), four (Ø6.5 mm) on the clavicle, and four (Ø14 mm) on the upper arm – two placed on anatomical landmarks (lateral and medial epicondyles) and two as far as possible from the deltoid. For the scapula, one marker (Ø14 mm) was fixed on the acromion. In addition, the scapula was covered with a regular grid of fifty-six markers (Ø6.5

mm); this number was determined so as to have enough markers to cover the scapula while limiting the time required to place them.

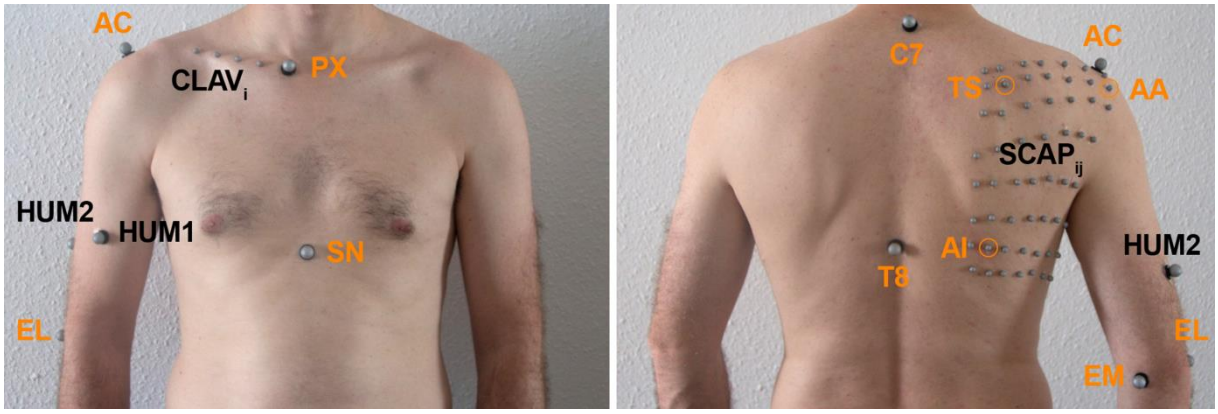

Figure 2: Markers placement, including markers placed on anatomical landmarks (orange) and technical markers (black). PX = xyphoid process, SN = sternal notch, AC = acromion, TS = trigonum spinae, AA = angulus acromialis, AI = angulus inferior, EL = lateral epicondyle, EM = medial epicondyle.

Kinematic data were collected simultaneously from an X-ray fluoroscopy unit (MultiDiagnostEleva, Philips Medical Systems, Netherlands) operating at 30 Hz and a Vicon MXT40S motion capture system (Vicon, Oxford Metrics, UK) consisting of eight cameras sampling at 120 Hz. Prior to data collection, the fluoroscopy system was calibrated for image distortion and radiographic projection parameters using a calibration object [13]. A calibration frame was also acquired with ten non-coplanar retroreflective markers, visible in both systems, to compute the pose of the coordinate system of the Vicon system relative to the fluoroscopy coordinate system by a 4×4 homogenous matrix. During testing, subjects were positioned in front of the fluoroscope with the torso at approximately 30° to the X-ray beam, so that the scapular plane was parallel to the image intensifier. They were instructed to perform two tasks: three consecutive flexions of the arm from neutral to maximum flexion, and three consecutive empty-can abductions of the arm from neutral to maximum abduction in the scapular plane. These standard movements were chosen because there have been widely investigated in the literature, facilitating comparison with previous studies. Subjects were not constrained during motion to allow natural arm movement.

2.4. Calculation of shoulder kinematics using X-ray fluoroscopy

The 3D poses of the scapula and humerus were obtained using a 3D-to-2D shape matching technique [14] (Fig. 3). The 3D MRI-based models were projected and iteratively matched to the 2D X-ray images using custom software. After manual initialization of the bones positions, a non-linear optimization algorithm based on an edge-to-edge metric was used to calculate the optimal poses of the bones. 3D clavicle and thorax motion was not determined because of the limited field of view of the fluoroscopy system (structures were not sufficiently visible). A previous validation study [15] had shown that best-case accuracy for fluoroscopy measurements was 0.53 mm for in-plane translation (parallel to image plane), 1.6 mm for out-of-plane translation (perpendicular to image plane), and 0.54° for rotations in all planes.

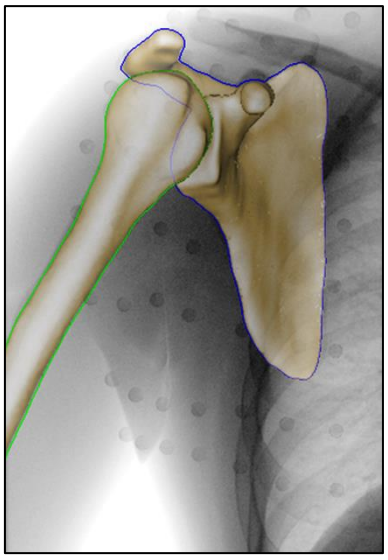

Figure 3: 3D-to-2D shape matching technique used to determine 3D motion of the scapula and humerus during dynamic arm movements.

2.5. Calculation of shoulder kinematics using skin markers

The main issue in estimating kinematics from skin markers is STAs: skin deformation and displacement due to the muscle activity cause parasitic marker movements with respect to the underlying bones [16]. Thus, rigid bone motion cannot be robustly estimated, unless STAs are effectively reduced. It was demonstrated that global optimization could help reduce overall STA error [8, 9]; this method minimizes overall STA error by taking account of the anatomical constraints of the entire kinematic chain. We therefore developed a patient-specific kinematic chain comprising four rigid bodies (thorax, clavicle, scapula and humerus) using the individual subject's 3D MRI-based models. The position and orientation of the thorax relative to the global coordinate system was determined with six degrees of freedom (DoF), and the sternoclavicular (SC), acromioclavicular (AC) and glenohumeral (GH) joints were each defined as ball-and-socket joint (3 DoF) with loose constraints on translation. Joint translation was thus permitted but limited.

The optimal pose of the kinematic chain was obtained by finding the best transform RT_s for each segment s that minimize the following equation:

$$min \sum_{s=1}^{4} \left(\sum_{i=1}^{n_s} \alpha_{si} \| RT_s x_{si} - y_{si} \|^2 \right) + \sum_{s=1}^{3} \beta_s \, \| t_s \|^2 \qquad (1)$$

This corresponds to the minimization of two terms:

- the distances between the model-based (x_{si}) and the measured (y_{si}) marker coordinates in the segment's cluster (n_s markers in segment's cluster s) with a weighting factor α_{si} to reflect different degrees of STA, as described by Lu and O'Connor [8];
- the translation penalty at each joint, with a weighting factor β_s to control the amount of possible translation at the joint and t_s the relative translation of the segment s with respect to its proximal bone.

For simplicity, equal weighting factors (α_{si}) were assigned to the markers of the thorax, clavicle and humerus clusters. Since STAs are significantly less in the flat portion of the

acromion [6], scapular grid markers were weighted inversely to their distance from the acromion. The weighting factors β_s were chosen to allow translation values of the same order of magnitude as reported in the literature.

Eq. (1) was solved using a non-linear sequential quadratic programming algorithm [17]. Figure 4 shows examples of computed motions.

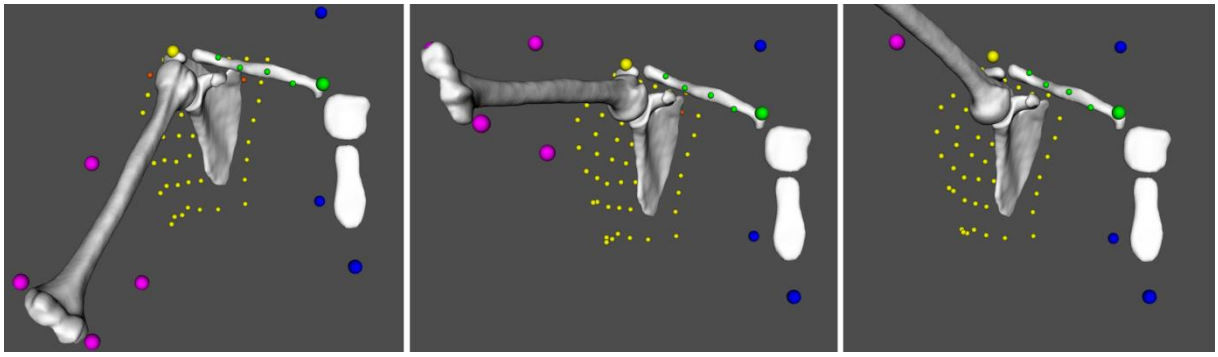

Figure 4: Kinematic animation of the shoulder joints during empty-can abduction, including the markers setup (small colored spheres).

2.6. Data analysis

Humeral motion with respect to the scapula was determined for both measurement methods with order of rotation: shoulder abduction/adduction (X_s), flexion/extension (Z', floating axis) and internal/external rotation (Y_h). This sequence was used because it is the best in terms of gimbal lock and amplitude coherence [18]. For the two motor tasks, the mean, standard deviation (SD) and root mean square error (RMSE) of the difference between the two measurement methods were calculated, as well as the motion amplitude (i.e., total measured motion) yielded from the fluoroscopic measurements.

3. Results

RMSEs for shoulder orientation were within 4° for each anatomical axis and each motion (Table 1). Minimal errors were observed for shoulder abduction/adduction and flexion/extension during flexion (mean ± SD: 2.0° ± 1.7° and 2.0° ± 2.4°, respectively). The range of glenohumeral translation was smallest in the superior-inferior direction (amplitude: 4.6 mm for flexion; 5.1 mm for abduction). Maximal amplitude reached 6 mm during abduction in lateral-medial direction. Mean error ranged between 1.9 and 3.3 mm. Maximum RMSE for flexion was 3.7 mm and 3.5 mm for empty-can abduction. Overall, orientation errors were lower for flexion, whereas translation errors were comparable for both motor tasks.

4. Discussion

We presented a patient-specific measurement technique based on the fusion of motion capture and MRI data. Kinematics was assessed using a patient-specific kinematic chain model of the shoulder complex with loose constraints on joint translation. To our knowledge, this methodology is the first attempt to calculate both rotation and translation at the shoulder joint based on skin-mounted markers.

Table 1

Mean ± SD errors, root mean square errors (RMSE) of shoulder kinematics between fluoroscopy-based and markers-based measurement. The motion amplitude (total measured motion) obtained from fluoroscopic measurement is also reported.

Movement	**Glenohumeral rotation**			
	Rotation (°)	Amplitude	Mean ± SD	RMSE
Flexion				
	Abduction/adduction (X)	105.0	2.0 ± 1.7	2.7
	Flexion/extension (Z)	53.5	2.0 ± 2.4	2.7
	Internal/external rotation (Y)	68.6	3.1 ± 2.5	3.9
Empty-can abduction				
	Abduction/adduction (X)	92.6	3.4 ± 2.3	4.0
	Flexion/extension (Z)	32.6	2.8 ± 2.2	3.5
	Internal/external rotation (Y)	54.2	3.1 ± 2.4	3.9

Movement	**Glenohumeral translation**			
	Translation (mm)	Amplitude	Mean ± SD	RMSE
Flexion				
	Anterior/posterior translation (X)	5.8	1.9 ± 1.2	2.2
	Lateral/medial translation (Z)	5.9	2.9 ± 1.6	3.3
	Superior/inferior translation (Y)	4.6	3.1 ± 2.1	3.7
Empty-can abduction				
	Anterior/posterior translation (X)	5.7	2.1 ± 1.8	2.8
	Lateral/medial translation (Z)	6.0	3.3 ± 1.3	3.5
	Superior/inferior translation (Y)	5.1	3.1 ± 1.5	3.5

Orientations RMSEs were within 4°, which is good and acceptable for clinical use in the study of shoulder pathology. For comparison, Karduna et al. [19] reported RMSEs of 10° for a scapula tracker and 11.4° for an acromial method against bone pins; Warner et al. [6] found RMSEs of 3.5° to 7.3° comparing an acromion marker cluster to a scapula locator. We were not able to find any comparative data in the literature specific to the relative motion of the humerus with respect to the scapula.

Difficulties were encountered in determining glenohumeral translation due to the great mobility of the joint. Although our data contained some significant translational errors, particularly in superior-inferior direction, the patterns of humeral translation were in good agreement with previous reports. For example, the data computed from the skin markers showed that the humeral head translated superiorly during the early phase of arm elevation and inferiorly toward maximum elevation (Fig. 5), as previously reported [14, 20]. Nevertheless, improvement is still needed. One direction could be to replace loose translational constraints with a full biomechanical simulation (e.g., finite element models) of the capsular ligaments taking account of their 3D shapes and mechanical properties.

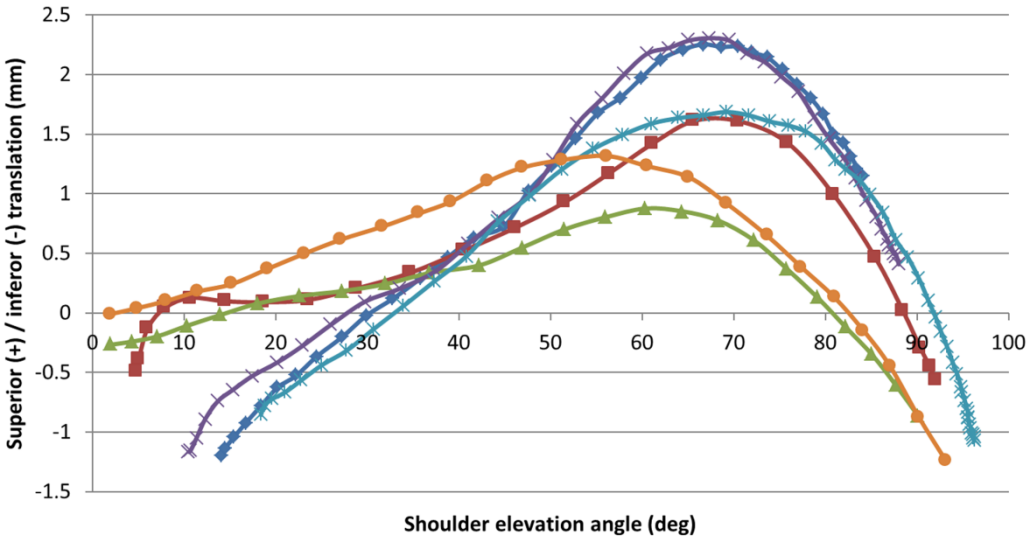

Figure 5: Superior-inferior translations of the humeral head as a function of shoulder elevation angle during empty-can abduction. Each curve corresponds to one of the six participants.

Two sources of errors that may contribute to the differences in shoulder kinematics as determined by fluoroscopy versus motion capture should be considered: Firstly, MRI-based models were used for the 3D-to-2D matching technique rather than CT-based models, which may have impaired the quality of the shape matching results [15]. MRI was chosen because we wanted to review soft-tissue lesions as part of a future study. Secondly, single-plane fluoroscopy provides poor measurement accuracy for out-of-plane translation. Biplane fluoroscopy provides smaller measurement errors [1], but subjects are exposed to twice as much radiation and the equipment is rarely available in a clinical setting.

5. Conclusion

The results of this study showed that the proposed technique could provide valuable kinematic data at the glenohumeral joint. Most importantly, we demonstrated that a first estimation of joint translation was feasible using an external measurement system, such as motion capture. This original technique may open new horizons leading to improved understanding of shoulder pathologies and opening up new possibilities of analyzing large ranges of shoulder motion, for instance during sports movements.

Disclosure of interest

The authors declare that they have no conflicts of interest concerning this article.

Acknowledgments

This work was supported by grants from La Tour Hospital, Geneva, Switzerland, and from the European Society of Shoulder and Elbow Surgery.

References

1. Zhu Z., Massimini D.F., Wang G., Warner J.J.P., Li G.. The accuracy and repeatability of an automatic 2D-3D fluoroscopic image-model registration technique for determining shoulder joint kinematics *Medical Engineering & Physics.* 2012;34:1303–1309.

2. Jackson M., B.Michaud , Tetreault P., Begon M.. Improvements in measuring shoulder joint kinematics *J Biomech.* 2012;45:2180–2183.

3. Klotz M.C.M., Kost L., Braatz F., et al. Motion capture of the upper extremity during activities of daily living in patients with spastic hemiplegic cerebral palsy *Gait & Posture.* 2012;38:148-152.

4. Johnson G.R., Stuart P.R., Mitchell S.. A method for the measurement of three-dimensional scapular movement *Clin Biomech.* 1993;8:269–273.

5. Andel C., Hutten K., Eversdijk M., Veeger D., Harlaar J.. Recording scapular motion using an acromion cluster *Gait & Posture.* 2009;29:123–128.

6. Warner M.B., Chappell P.H., Stokes M.J.. Measuring scapular kinematics during arm lowering using the acromion marker cluster *Hum Mov Sci.* 2012;31:386–396.

7. Mattson J.M., S.A.Russo , Rose W.C., K.M.Rowley , J.G.Richards . Identification of scapular kinematics using surface mapping: A validation study *J Biomech.* 2012;45:2176–2179.

8. Lu T.W., O'Connor J.J.. Bone position estimation from skin marker co-ordinates using global optimisation with joint constraints *J Biomech.* 1999;32:129–134.

9. Roux E., Bouilland S., Godillon-Maquinghen A.-P., Bouttens D.. Evaluation of the global optimisation method within the upper limb kinematics analysis *J Biomech.* 2002;35:1279–1283.

10. Yushkevich P.A, Piven J., Hazlett H.C., et al. User-Guided 3D Active Contour Segmentation of Anatomical Structures: Significantly Improved Efficiency and Reliability *Neuroimage.* 2006;31:1116–1128.

11. Wu G., Helm F.C.T., Veegerc H.E.J., et al. ISB recommendation on definitions of joint coordinate systems of various joints for the reporting of human joint motion - part II: shoulder, elbow, wrist and hand *J Biomech.* 2005;38:981–992.

12. Schneider P.J., Eberly D.H.. *Geometric Tools for Computer Graphics*. The Morgan Kaufmann Series in Computer Graphics and Geometric Modeling 2003.

13. Lu T.W., Tsai T.Y., Kuo M.Y., Hsu H.C., Chen H.L.. In vivo three-dimensional kinematics of the normal knee during active extension under unloaded and loaded conditions using single-plane fluoroscopy *Med Eng & Phys.* 2008;30:1004–1012.

14. Matsuki K., Matsuki K.O., Yamaguchi S., et al. Dynamic In Vivo Glenohumeral Kinematics During Scapular Plane Abduction in Healthy Shoulders *J Orthop Sports Phys Ther.* 2012;42:96–104.

15. Moro-oka T., Hamai S., Miura H., et al. Can Magnetic Resonance Imaging–Derived Bone Models Be Used for Accurate Motion Measurement with Single-Plane Three-Dimensional Shape Registration *J Ortho Res.* 2007;25:867–872.

16. Leardini A., Chiari L., Croce U. Della, Cappozzo A.. Human movement analysis using stereophotogrammetry Part 3: Soft tissue artifact assessment and compensation *Gait & Posture.* 2005;21:212–225.

17. Lawrence C.T., Tits A.L.. A Computationally Efficient Feasible Sequential Quadratic Programming Algorithm *SIAM J Optim.* 2001;11:1092–1118.

18. Bonnefoy-Mazure A., Slawinski J., Riquet A., J.-M.Lévèque , Miller C., Chèze L.. Rotation sequence is an important factor in shoulder kinematics. Application to the elite players' flat serves *J Biomech.* 2012;43:2022–2025.

19. Karduna A.R., McClure P.W., Michener L.A., Sennett B.. Dynamic measurements of three-dimensional scapular kinematics: a validation study *J Biomech Eng.* 2001;123:184–190.

20. Massimini D.F., Boyer P.J., Papannagari R., Gill T.J., Warner J.P., Li G.. In-vivo glenohumeral translation and ligament elongation during abduction and abduction with internal and external rotation *J Orthop Surg Res.* 2012;7:29–38.